A BIOINTERFACE GROWTH AT IMMERSION OF A BIODEGRADABLE MAGNESIUM ALLOY IN SIMULATED BODY FLUID

Manuela-Elena VOICU[1], Florentina GOLGOVICI[2]

The bioactivity of the AZ31 magnesium alloy was tested "in vitro", following the evolution of the apatite layers developed on the surface of the samples after immersion in SBF through surface analysis and electrochemical testing. The morphological surface analysis was performed by scanning electron microscopy (SEM), the structure of the deposited layer was analyzed by Fourier transform infrared spectroscopy (FT-IR) and the concentration of metal ions released in the SBF solution was measured using an inductively coupled plasma mass spectrometer (ICP-MS).

Keywords: biodegradable alloy, electrochemical stability, SEM, SBF, ICP-MS

1. Introduction

The most common metallic implant biomaterials [1] are based on stainless steel, CoCr and Ti alloys [2]. The main properties required for their use in bio-applications are electrochemical stability in bioliquids [3, 4], good mechanical behavior [5] and biocompatibility [6]. Various treatments and processing were applied to the biomedical alloys to enhance their performance [7, 8].

An interesting approach tries to mimic nature by creating and manipulating bioinspired structures at micro and nano level leading to new advanced construct in tissue engineering combining and treating traditional biomaterials [9, 10].

Usually, in a majority of applications that include implant use, there is a need to reduce the corrosion of metallic biomaterials, but more recently the interest to use corrodible metals in temporary implants is increasing [11]. This fact is due to development of "biodegradable metals" which are firstly represented by Mg-based, Fe-based and Ca binary and ternary alloys [12].

The investigation of such bioactive metals started with their structures, mechanical and degradation aspects, "in vitro" and "in vivo" tests, pre-clinical and clinical performances [13, 14].

[1] PhD Student, Dept. of General Chemistry, University POLITEHNICA of Bucharest, Romania, e-mail: manuela.voicu94@gmail.com

[2] Assoc. Prof., Dept. of General Chemistry, University POLITEHNICA of Bucharest, Romania, e-mail: florentina.golgovici@upb.ro

Nowadays, the strategy of controlling and monitoring their biodegradation rates after surface modifications *via* various procedures is one of the important challenges in implant research [15, 16].

Magnesium alloys are recognized as alternatives to other implant alloys not only for biodegradability but for their lower weight and high strength-to-weight ratio as well. Pitting corrosion appears on the magnesium in the presence of chloride ions. They transform the protective $Mg(OH)_2$ into soluble $MgCl_2$ thus accelerating the dissolution of magnesium [17].

The main objective of this paper was to study the behavior of a biodegradable MgAlZn alloy in SBF solution, due to the possibility to be used as temporary implant. The behavior of AZ31 alloy followed for long periods, as well as the study of the morphology and composition of the resulting products are the novelties of this research.

2. Experimental

The AZ31 magnesium alloy, with a ratio of 96:3:1, was provided by *Alfa Aesar, ThermoFisher, Kandel Germany*, in the form of a foil with the dimensions 30×30×1 mm. For all experiments, the MgAlZn foil was cut into 2×2 cm samples. Five samples were polished using SiC abrasive paper with increasing grain size up to 1200 and then they were cleaned and degreased using 96% vol. Ethyl alcohol (*Chimreactiv SRL, Bucharest*) for 10 minutes in the ultrasonic bath.

Then, the samples were removed and left to dry on filter paper in air.

The simulated body fluid (SBF) Kokubo used had the composition shown in table 1.

Table 1

Composition of SBF solution [18]

Component	NaCl	$NaHCO_3$	KCl	$K_2HPO_4 \cdot 3H_2O$	$MgCl_2 \cdot 6H_2O$	$CaCl_2$	Na_2SO_4	$(CH_2OH)_3CNH_2$
Concentration, g/L	7.996	0.350	0.224	0.228	0.305	0.278	0.071	6.057

The bioactivity of the samples was tested ”in vitro”, following the evolution of the apatite layers developed on the surface of the samples after immersion in SBF through surface analysis and electrochemical testing.

A 3.6 cm^2 surface of the working electrode was immersed in the SBF solution.

Each alloy plate was immersed in a volume of SBF solution, in 5 sterile containers, kept for 1 day, 3 days, 7 days, 21 days and 28 days.

After each immersion time, both the SBF solution and the AZ31 magnesium alloy samples were tested.

The surface analysis was performed by scanning electron microscopy (SEM) before and after different immersion times in the SBF using a microscope provided by FEI, model Quanta 650 FEG, together with beam analysis module X-ray energy dispersion (EDX).

The structure of the deposited layer that identified the appearance and evolution of the phosphate film was analyzed by Fourier transform infrared spectroscopy (FT-IR) with the PerkinElmer Spectrometer, between 4000 and 600 cm^{-1}, at a resolution of 0.5 cm^{-1}.

The concentration of metal ions released in the SBF solution was measured using an inductively coupled plasma mass spectrometer (ICP-MS) from Perkin Elmer, model ELAN DRC-e.

Electrochemical methods

The corrosion resistance of the MgAlZn alloy has been tested with the following electrochemical methods: open-circuit electrical potential (OCP); electrochemical impedance spectroscopy (EIS); linear potentiodynamic polarization (Tafel plots).

The electrochemical methods were performed using an AutoLab PGSTAT 12 EcoChemie potentiostat/galvanostat.

On this line, the determinations were made using an electrochemical cell with three electrodes: an Ag/AgCl electrode as reference electrode (RE); a platinum (Pt) counter-electrode (EC) and MgAlZn plate as working electrode (WE). Potentiodynamic curves were recorded by polarizing the AZ31 sample at $2mVs^{-1}$ scan rate. Electrochemical impedance spectroscopy tests were performed at open circuit potential by application of 10mV amplitude ac voltage in the frequency range between 10 kHz and 0.01 Hz. The impedance data were analyzed using Nyquist and Bode plots.

3. Results and discussion

3.1. SEM characterization

The evolution of the morphology at different periods of time is reproduced by the SEM images in Fig. 1. The SEM images show the morphology of the surfaces of the samples analyzed at a magnification of 20000X.

On the surface of the uncoated Mg sample, scratches can be observed which the results of polishing are. Small formations that are probably magnesium oxide (MgO) crystals can be observed (Fig. 1a).

Compared to uncoated Mg alloy, after 1 day of immersion in SBF solution (Fig. 1b) on the alloy surface a coating can be observed. The base size of crystals deposited on magnesium alloy surface is about 200 nm, also agglomerations of crystals can be observed.

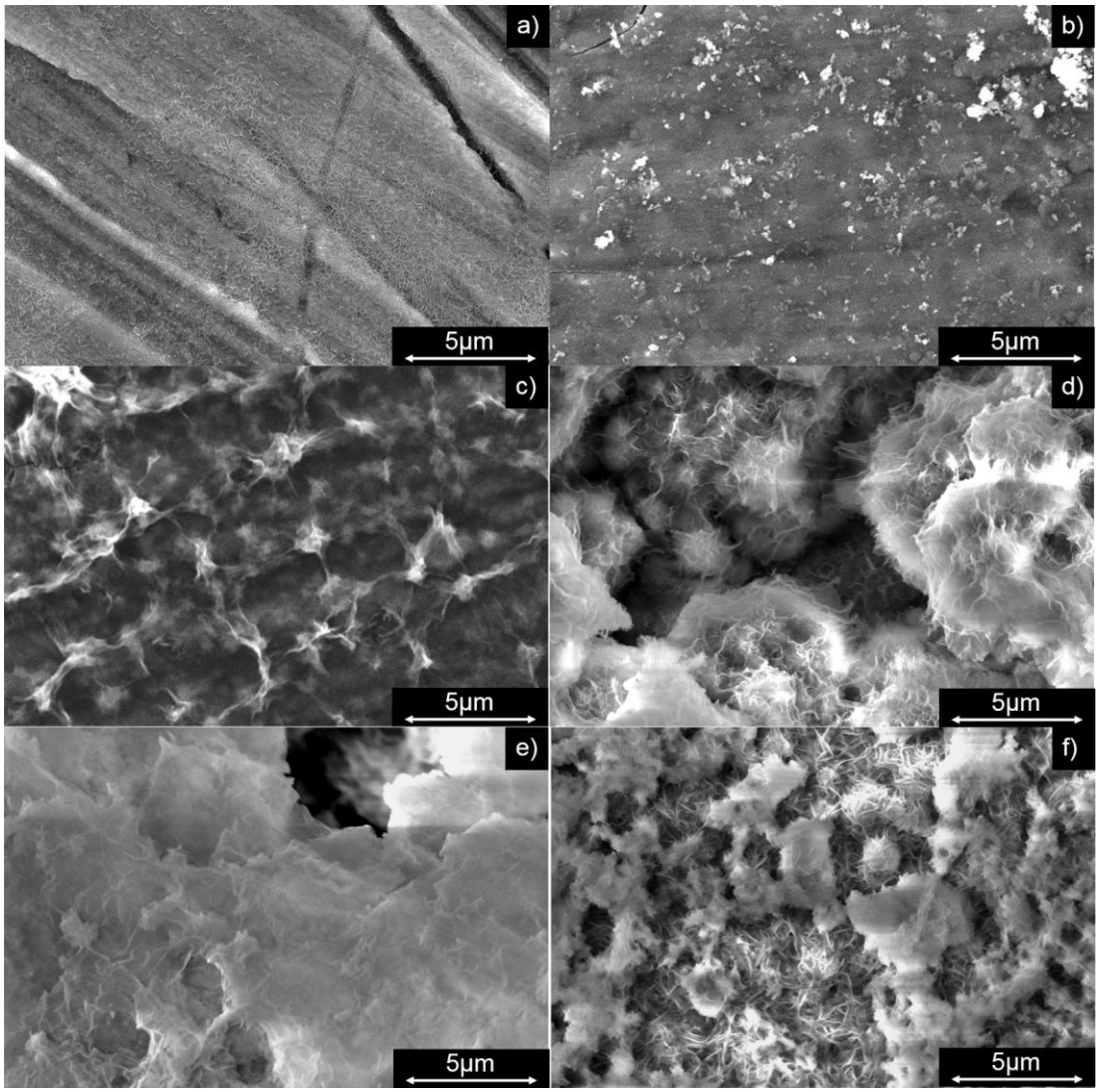

Fig. 1. SEM image of a) uncoated Mg alloy and after: b) 1 day, c) 3 days, d) 7 days, e) 21 days, f) 28 days immersion in SBF solution

At 3 days of immersion (Fig. 1c), the deposited crystals have a semi-self-organized network form with a central formation with a diameter of about 1.5 μm and branches with lengths of 2-4 μm.

After 7 days of immersion (Fig. 1d), on the surface of the sample are observed crystals with a specific form of calcium phosphate, with varying sizes between 2 and 10 μm. At 21 days (Fig. 1e), on the sample can be observed only crystals of irregular shapes and dimensions of the order of tens of μm can be observed.

From geometrical point of view, after 28 days (Fig. 1f), two types of crystals can be observed, a cross-linked type, possibly of calcium phosphate, and a cubic type, possibly of sodium or calcium chloride. The dimensions of the lattice crystals are about 500 nm long and 50 nm wide and the side length of a basic cubic crystal is also about 500 nm. On the surfaces of the Mg alloy samples, hydroxyapatite was observed as crystals after immersion in the SBF solution. The EDX analysis (Fig. 2 and table 2) highlight the evolution of the composition of the coatings on the samples after the immersion.

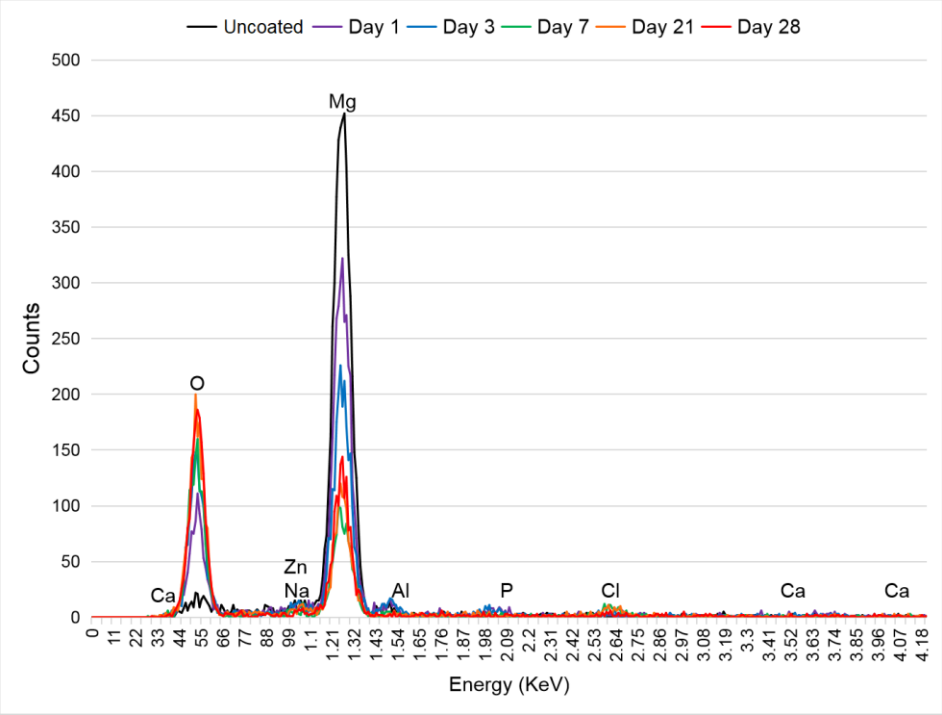

Fig. 2. EDX image of uncoated Mg alloy and after 1 day, 3 days, 7 days, 21 days, 28 days immersion in SBF solution

Table 2

The evolution in time of the elements detected in the deposits on the alloy

Items / Immersion time	Mass %					
	Uncoated	1 day	3 days	7 days	21 days	28 days
O	3.18	17.9	30.86	47.53	49.61	49.02
Na	-	0.50	2.88	2.42	2.19	0.78
Mg	96.82	77.69	56.73	37.49	39.56	43.93
P	-	1.46	2.60	1.33	0.68	0.87
Cl	-	-	-	7.58	6.3	1.85
Ca	-	-	2.15	1.87	1.65	2.85

The uncoated sample contains a small amount of oxygen, an indicator that magnesium has partially oxidized in the atmosphere. The immersion of the samples led to the deposition of salts from the SBF solution on the surface of the magnesium alloy. The evolution of the deposits indicates that the first compounds that are deposited on the surface are those containing sodium (Na) and phosphorus (P). On day 7, the atomic ratio Ca/P is 1.4, and this is very close to the ratio found in hydroxyapatite which is generally accepted as 1.67.

3.2. FT-IR tests

The infrared spectra of the magnesium alloy coated at various immersion times (Fig. 3) showed absorption of infra-red light in various band which indicates the presence of functional group like phosphate (980-1190 cm^{-1}) and hydroxyl (635-3570 cm^{-1}).

The peaks from 3350 cm^{-1}, as well as the one from 3690 cm^{-1}, are attributed to the vibration motion of hydroxyl (OH^-) functional groups.

The carbonate band ($CO3^{2-}$) was detected at 1410 cm^{-1} and indicates that the hydroxyapatite structure contains carbonate ion [19].

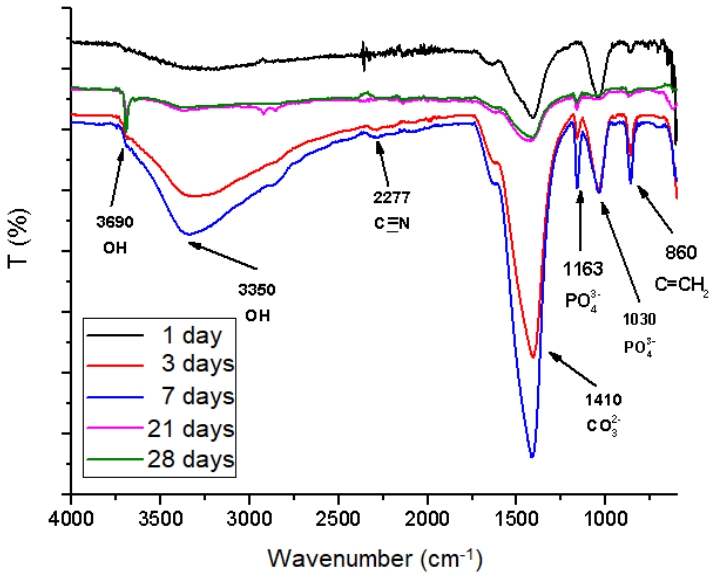

Fig. 3. FT-IR spectra of MgAlZn alloy samples investigated at various immersion times

3.3. ICP-MS measurements

Table 3 shows the evolution of the concentration of Ca^{2+} and Mg^{2+} over time. The ICP-MS analysis shows that, over time, the amount of Mg^{2+} in the SBF solution decreases due to the possible formation on the surface of the alloy of a magnesium oxide (MgO) which increases in thickness proportional to the number

of days immersed in SBF. Hydroxyapatite formation on magnesium alloy it indicated by the decrease of Ca^{2+} ions amount in SBF solution.

Table 3

Concentration of Ca^{2+} and Mg^{2+} over time

Immersion time, days	Items analyzed	
	Ca^{2+}, mg/L	Mg^{2+}, mg/L
1	7.698	87.497
3	6.862	67.108
7	6.569	48.519
21	3.94	18.605
28	4.107	14.737

3.4. OCP determination

Open circuit potential (OCP) measurements were made during 10 minutes.

As we can see in Fig. 4, in a first step, the potentials value shift rapidly towards electropositive values in the first seconds of immersion in SBF electrolyte. However, a second phase in which the potential values shift towards electropositive values is slower, ending with a plateau. These trends suggest that on the alloy increases continuously a surface passive film and the emergence of a relatively stable potential is an indication of stable chemical nature of this passive film. As itcan be observed from Fig. 4, the stable value of the reached potential has increasingly electropositive values as the immersion time of the magnesium alloy in SBF solution increases.

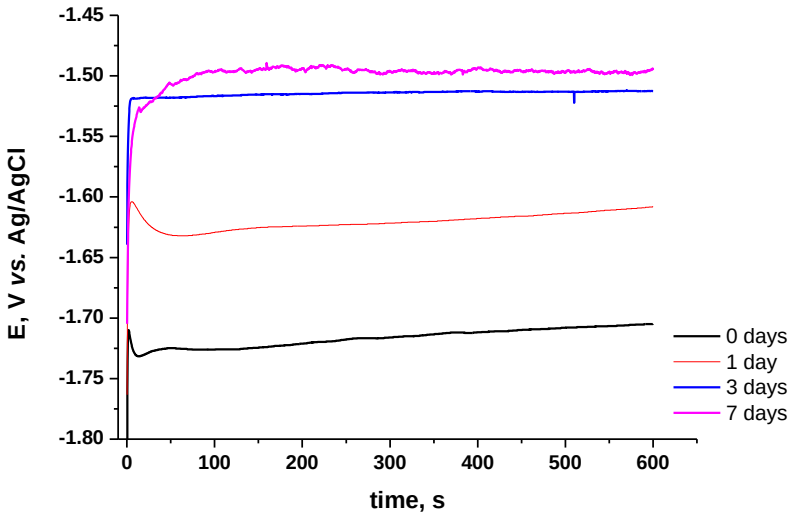

Fig. 4. OCP variation for magnesium alloy after different immersion time in SBF

3.5. EIS tests

Electrochemical impedance spectroscopy (EIS) tests for AZ31 alloy in SBF have led to the recording of the spectra presented in the Nyquist and Bode diagrams (Fig. 5). From Nyquist diagrams (Fig. 5a), the presence of two open capacitive semicircles can be observed for magnesium alloy immediately after immersion in SBF solution. For AZ31 alloy after 1, 3 and 7 immersion days, only one capacitive semicircle appears. The diameters of semicircles increase with immersion time, indicating an increase in polarization resistance, which leads to a decrease of the corrosion rate. The Nyquist plots show that an inductive loop is seen in all samples at low frequencies. The Bode diagram (Fig. 5b) reveals the presence of a two time constants corresponding to semicircles from the Nyquist diagrams. The first maximum phase angle value is recorded at high frequency, while the second maximum phase angle is obtained at lower frequency. After immersion in SBF, the Bode diagram reveals the presence of a single time constant corresponding to a single semicircle on the Nyquist diagrams. The maximum phase angle moves to lower frequencies and increases slightly once the immersion time in the SBF solution increase. The increase of the maximum phase angle values from -44 to -60^{o}, indicate the formation of a protective film on alloy surface, which results in an almost capacitance response of the interface.

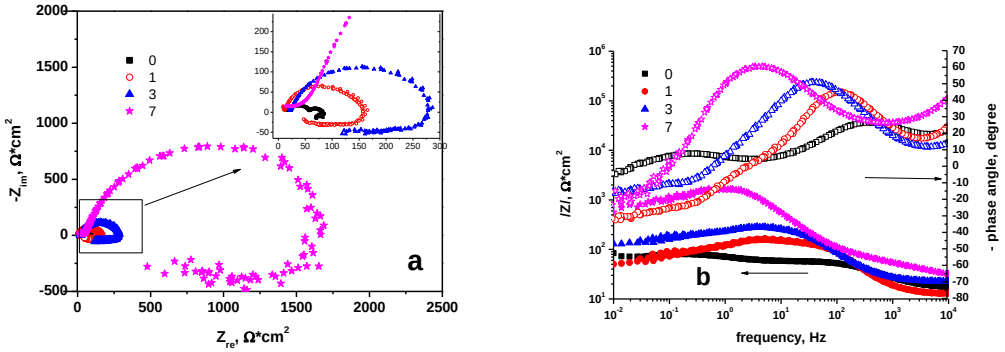

Fig. 5. a) Nyquist and b) Bode diagrams for AZ31 alloy after different immersion time at OCP in SBF

Therefore, magnesium is protected by sulphates, phosphates and carbonates formed in time in the SBF solution.

3.6. Linear potentiodynamic polarization (Tafel plots)

The polarization curves (shown in Fig. 6) were recorded after different immersion time in electrolyte in order to observe the behavior of AZ31 alloy in SBF. The anodic oxidation of magnesium alloy can be observed on the anodic branch of polarization curves. As can be seen, two different slopes appear on the anodic polarization curves, this indicate a kinetic barrier effect, due to deposition

of a protective layer on magnesium alloy surface followed by its dissolution at more electropositive values of potential. The decrease of the corrosion current density values, once the immersion time increase, it can be observed. These can be explained by the formation of a protective film on alloy surface, which leads to slower corrosion of this alloy. Also, a shift of corrosion potential towards electropositive values with increase of immersion time can be seen from Fig. 6. From polarization curves (Fig. 6) the kinetic parameters were calculated using two methods: the Tafel slopes and corrosion resistance.

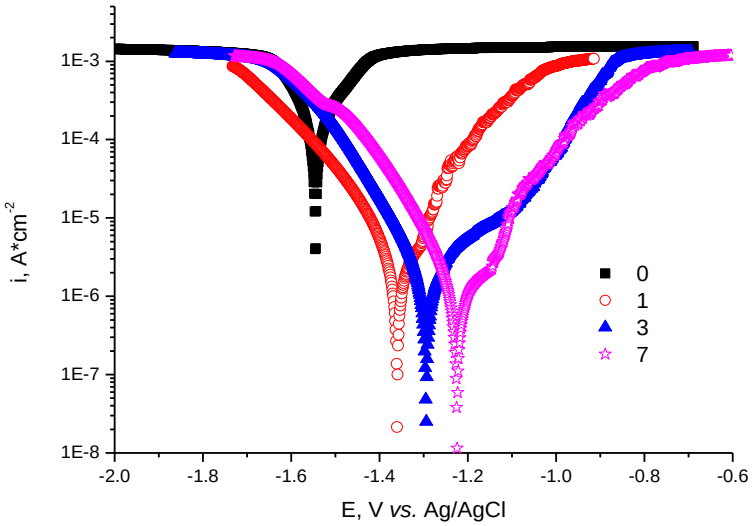

Fig. 6. Polarization curves for AZ31 alloy in SBF at different immersion time

The values obtained for the corrosion potential (E_{corr}), the corrosion current density (i_{corr}), the gravimetric index (K_g), the penetration index (P), polarization resistance (R_P) are shown in Table 4.

Table 4

Corrosion kinetic parameters for AZ31 alloy at different immersion times in SBF

Immersion time, days	Tafel slope method					Polarization resistance method	
	E_{corr}, V	i_{corr}, μA/cm^2	R_{mpy}	K_g, g/m^2 h	P, mm/year	R_p, Ω	i_{corr}, μA/cm^2
0	-1.54	362	173.39	4.122	4.4009	52	391.75
1	-1.52	2.97	1.422	0.0338	0.0361	4710	4.56
3	-1.29	1.61	0.771	0.0183	0.0196	6771	2.61
7	-1.22	0.54	0.258	0.0062	0.0065	8524	1.75

As we can see from Table 4, the two methods yield a similar value of the corrosion current density. The increase of the immersion time in SBF solution leads to the decrease of the corrosion rate as well as to the polarization resistance increase.

4. Conclusions

To conclude, we have described the behavior of biodegradable AZ 31 magnesium in SBF solution. An interface grown during the immersion of magnesium alloy in simulated body fluid was investigated in time by morphological, structural and electrochemical point of view. Appearance and growth on the magnesium alloy surface of MgO, hydroxyapatite or hydroxyapatite precursors was highlighted by FTIR, SEM, ICP-MS analysis. The electrochemical behavior of AZ31 magnesium alloy in SBF solution was investigated by potentinodynamic polarization and electrochemical impedance spectroscopy tests. The formation of a protective film on alloy surface has been confirmed by the increase of the maximum phase angle values from -44 to -60^{o}, when the immersion time in the SBF increases. Based on experimental data it has been established that the immersion time increase in SBF solution leads to the decrease of the corrosion rate as well as to the polarization resistance increase. Potentiodynamic polarization test have confirmed the data obtained from EIS measurements.

The investigations support the use of biodegradable AZ31 magnesium alloy as implants.

Acknowledgements

The work was supported by Romanian Ministry of Education and by Executive Agency for Higher Education, Research, Development and Innovation Funding, under UEFISCDI 65PCCDI/2018 - REGMED.

R E F E R E N C E S

[1]. *M. Niinomi*, Metallic biomaterials, Journal of Artificial Organs, **Vol. 11,** Issue 3, 2008, pp. 105-110;

[2]. *M. Vardaki, M. Prodana, A. B. Stoian, D. Ionita,* Corrosion and bioactivity of a bioinspired coating on tizr alloys, UPB Scientific Bulletin, Series B: Chemistry and Materials Science, **Vol. 80**, Issue 1, January 2018, pp. 209-216;

[3]. *M. Popa, I. Demetrescu, E. Vasilescu, P. Drob, D. Ionita, C. Vasilescu*, Stability of some dental implant materials in oral biofluids, Revue Roumaine de Chimie, **Vol. 50**, Issue 5, 2005, pp. 399-406;

[4]. *M. V. Popa, D. Iordachescu, I. Demetrescu, E. Vasilescu, P. Drob, A. Cimpean, M. Istratescu, C. Vasilescu*, The relation between electrochemical tests and in vitro evaluation of titanium alloy biocompatibility, Materials and Corrosion, **Vol. 58**, Issue 9, 2007, pp. 687-695;

[5]. *T. Nakano*, Mechanical properties of metallic biomaterials, Metals for Biomedical Devices, Woodhead Publishing Series in Biomaterials, 2010, pp. 71-98;

[6]. *M. Niinomi*, Design and development of metallic biomaterials with biological and mechanical biocompatibility, Journal of Biomedical Materials Research, **Vol. 107**, Issue 5, 2019, pp. 944-954;

[7]. *M. Mindroiu, E. Cicek, F. Miculescu, I. Demetrescu*, The influence of thermal oxidation treatment on the electrochemical stability of TiAlV and TiAlFe alloys and their potential application as biomaterials, Revista de Chimie, **Vol. 58**, Issue 9, 2007, pp. 898-903;

[8]. *J. Izquierdo, G. Bolat, N. Cimpoesu, L. C. Trinca, D. Mareci, R. M. Souto*, Electrochemical characterization of pulsed layer deposited hydroxyapatite-zirconia layers on Ti-21Nb-15Ta-6Zr alloy for biomedical application, Applied Surface Science, **Vol. 385**, November 2016, pp. 368-378;

[9]. *P. Fratzl*, Biomimetic materials research: what can we really learn from nature's structural materials?, Journal of The Royal Society Interface, **Vol. 4** Issue 15, September 2007, pp. 637-642;

[10]. *A. B. Stoian, I. Demetrescu, D. Ionita*, Nanotubes and nano pores with chitosan construct on TiZr serving as drug reservoir, Colloids and Surfaces B: Biointerfaces, **Vol. 185**, 1 January 2020, 110535;

[11]. *J. V. Rau, I. Antoniac, M. Fosca, A. De Bonis, A. I. Blajan, C. Cotrut, V. Graziani, M. Curcio, A. Cricenti, M. Niculescu, M. Ortenzi, R. Teghil*, Glass-ceramic coated Mg-Ca alloys for biomedical implant applications, Materials Science and Engineering: C, **Vol. 64**, 1 July 2016, pp. 362-369;

[12]. *Y. F. Zheng, X. N. Gu, F. Witte*, Biodegradable metals, Materials Science and Engineering R: Reports, **Vol. 77**, March 2014, pp 1-34;

[13]. *F. Witte, V. Kaese, H. Haferkamp, E. Switzer, A. Meyer-Lindenberg, C. J. Wirth, H. Windhagen*, In vivo corrosion of four magnesium alloys and the associated bone response, Biomaterials, **Vol. 26**, Issue 17, 2005, pp. 3557-3563;

[14]. *M. Prakasam, J. Locs, K. S. Ancane, D. Loca, A. Largeteau, L. B. Cimdina*, Biodegradable Materials and Metallic Implants-A Review, Journal of Functional Biomaterials, **Vol. 8**, Issue 4, 2017;

[15]. *R. Hedayati, S. M. Ahmadi, K. Lietaert, N. Tumer, Y. Li, S. A. Yavari, A. A. Zadpoor*, Fatigue and quasi-static mechanical behavior of bio-degradable porous biomaterials based on magnesium alloys, Journal of Biomedical Materials Research Part A, **Vol. 106**, Issue 7, February 2018, pp. 1798–1811;

[16]. *H. Moldovan, E. Plopeanu, G. Dan, M. Vasilescu, M. Dobrescu, C. Milea, K. Earar, D. Gheorghita*, Contributions on biodegradability of Mg-Ca alloys for orthopedic implants, UPB Scientific Bulletin, Series B: Chemistry and Materials Science, **Vol. 80**, Issue 4, January 2018, pp. 229-246;

[17]. *G. Song*, Control of biodegradation of biocompatable magnesium alloys, Corrosion Science, **Vol. 49**, Issue 4, April 2007, pp. 1696-1701;

[18]. *T. Kokubo, H. Kushitani, S. Sakka, T. Kitsugi, T. Yamamuro,* Solutions able to reproduce in vivo surface-structure changes in bioactive glass-ceramic A-W, Journal of Biomedical Materials Research, **Vol. 24**, Issue 6, 1990, pp. 721-734;

[19]. *S. Raynaud, E. Champion, D. Bernache-Assollant, P. Thomas,* Calcium phosphate apatites with variable Ca/P atomic ratio I. Synthesis, characterisation and thermal stability of powders, Biomaterials, **Vol. 23**, Issue 4, 15 February 2002, pp. 1065-1072.